Heterogeneous Catalysis

DOI: 10.1002/ange.201201737

A Noble-Metal-Free Catalyst Derived from Ni-Al Hydrotalcite for Hydrogen Generation from $N_2H_4{\cdot}H_2O$ Decomposition**

*Lei He, Yanqiang Huang, Aiqin Wang, Xiaodong Wang, Xiaowei Chen, Juan José Delgado, and Tao Zhang**

Storing hydrogen safely and efficiently is one of the major technological barriers preventing the widespread application of hydrogen-fueled cells, such as proton exchange membrane fuel cells (PEMFCs). Hydrous hydrazine ($N_2H_4{\cdot}H_2O$) is considered as a promising liquid hydrogen storage material owing to the high content of hydrogen (7.9%) and the advantage of CO-free H_2 produced.[1] In particular, hydrous hydrazine offers great potential as a hydrogen storage material for some special applications, such as unmanned space vehicles and submarine power sources, where hydrazine is usually used as a propellant.

The decomposition of hydrazine proceeds by two typical reaction routes:[2]

$$H_2NNH_2 \rightarrow N_2(g) + 2\,H_2(g) \quad (1)$$

$$3\,H_2NNH_2 \rightarrow 4\,NH_3(g) + N_2(g) \quad (2)$$

Reaction (2) not only decreases the yield of H_2 but also complicates the separation process of products, because the ammonia by-product would poison the Nafion membrane and the fuel-cell catalysts. Thereby, it is of crucial importance to develop a highly selective catalyst over which the reaction proceeds only by pathway (1) at low temperatures. To this end, Xu and co-workers[3] synthesized a series of nickel-containing bimetallic nanoparticles, including Ni-Rh, Ni-Pt, and Ni-Ir, which showed high H_2 selectivity at room temperature. Nevertheless, the incorporation of noble metals to nickel greatly increased the cost of catalysts. In a subsequent study by Xu and co-workers,[4] Ni-Fe nanoparticles were employed as catalysts for this reaction. However, the nanoparticles were only active at 70 °C, and addition of 0.5 mol L^{-1} NaOH was necessary for the high selectivity. Moreover, the practical application of colloidal nanoparticles will raise significant problems, such as mass production, handling, stability, separation, and recyclability. Therefore, from the viewpoint of practical applications, a supported base metal catalyst is a preferred choice owing to its low cost, good mechanical stability, and easy separation from the reaction medium.

Herein, using a Ni-Al hydrotalcite-like compound (Ni-Al-HT) as the precursor, we obtained a highly dispersed nickel catalyst that presented 100% conversion of $N_2H_4{\cdot}H_2O$ and up to 93% selectivity to H_2 for the decomposition of $N_2H_4{\cdot}H_2O$ at ambient temperature. To our knowledge, this is the first report in which supported base metal catalysts show such high selectivity towards the formation of H_2.

It is well-known that supported noble metal catalysts, especially iridium catalysts, are very active for the decomposition of hydrazine. Compared with Ir, Ni is less active.[5] Accordingly, to obtain a high activity over Ni catalysts, a very high loading of Ni is required while maintaining a high degree of dispersion. Hydrotalcite-like compounds have been demonstrated to be excellent precursors for the preparation of highly dispersed and high-loading metal catalysts.[6] Herein, we synthesized binary Ni-Al-HT with interlayer CO_3^{2-} anions by a co-precipitation method.[7] After reduction in a H_2 atmosphere at 500 °C, the sample was transformed into a highly dispersed Ni/Al_2O_3 nanocatalyst (denoted as Ni-Al_2O_3-HT). The molar ratio of Ni to Al, determined by ICP analysis, was 3:1. The BET surface areas of the Ni-Al-HT precursor and the derived Ni-Al_2O_3-HT catalyst were 248 $m^2 g^{-1}$ and 179 $m^2 g^{-1}$, respectively. The reduced Ni-Al_2O_3-HT catalyst was then transferred into deionized water without exposure to air and used for reaction without further treatment. The reaction was initiated by introducing $N_2H_4{\cdot}H_2O$ into the reactor containing the catalyst. Gaseous products released during the reaction were measured volumetrically and analyzed on-line with a gas chromatograph.[8] The selectivity to H_2 was evaluated based on Equations (1) and (2). For comparison, a traditional supported Ni/Al_2O_3 catalyst was also prepared by the impregnation method with the same amount of Ni loading (denoted as 78 wt% Ni/Al_2O_3-IMP). The synthesis details can be found in the Supporting Information.

Powder X-ray diffraction patterns (Figure 1a) illustrate the crystalline nature of the layered double hydroxide (LDH) structure of hydrotalcite. No other crystalline phases were detected, thus suggesting the high purity of the precursor.

[*] L. He, Dr. Y. Huang, Dr. A. Wang, Dr. X. Wang, Prof. T. Zhang
State Key Laboratory of Catalysis, Dalian Institute of Chemical Physics, Chinese Academy of Sciences
Dalian, 116023 (China)
E-mail: taozhang@dicp.ac.cn
Homepage: http://www.taozhang.dicp.ac.cn
L. He
Graduate University of Chinese Academy of Sciences
Beijing (China)
Dr. X. Chen, Dr. J. J. Delgado
Departamento de Ciencia de los Materiales e Ingeniería Metalúrgica y Química Inorgánica Facultad de Ciencias, Universidad de Cádiz
Puerto Real, Cadiz (Spain)

[**] The authors thank Prof. Qiang Xu and Prof. Jun Li for helpful discussions. This work was supported by the National Natural Science Foundation of China (21076211, 21103173, 21176235). Xiaowei Chen is grateful for the "Ramón y Cajar" program from the Spanish Ministry of Science and Innovation.

Supporting information for this article is available on the WWW under http://dx.doi.org/10.1002/anie.201201737.

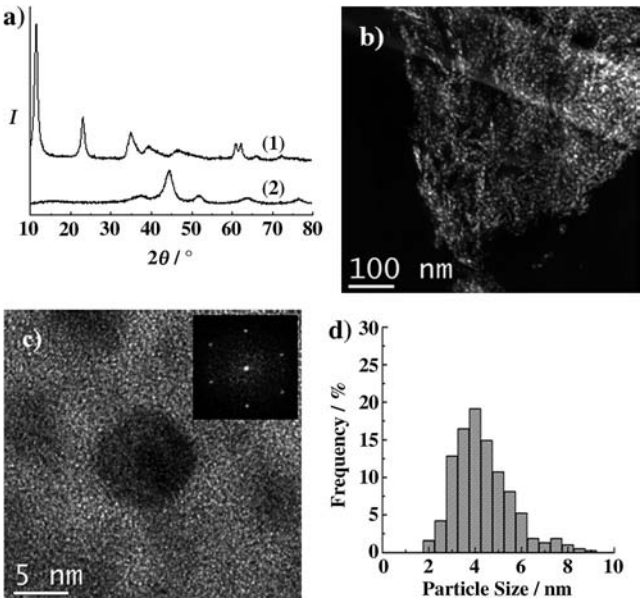

Figure 1. a) XRD patterns of: (1) Ni-Al-HT structure; (2) Ni-Al_2O_3-HT reduced at 500 °C. b) HAADF image for Ni-Al_2O_3-HT reduced at 500 °C. c) HRTEM image (inset: SAED) for a single particle. d) Histogram of the Ni particle size distribution.

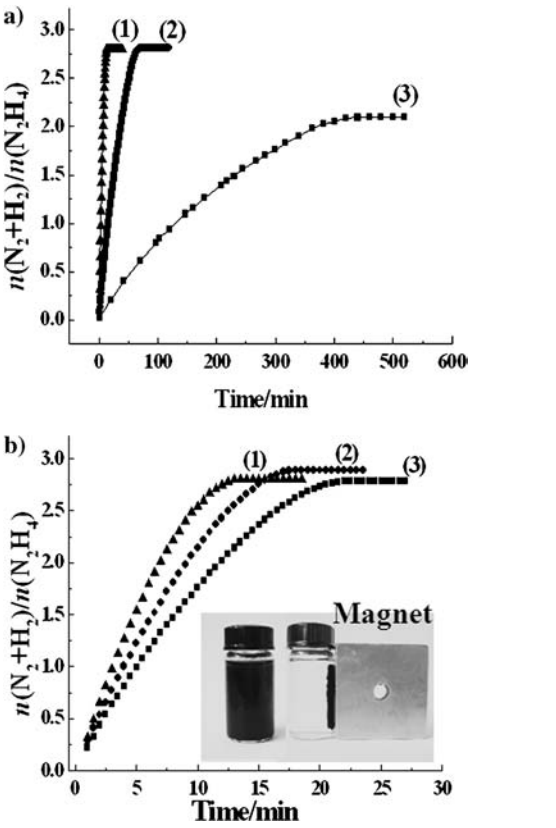

Figure 2. a) $n(N_2+H_2)/n(N_2H_4)$ versus time for Ni-Al_2O_3-HT and 78 wt% Ni/Al_2O_3-IMP at different reaction temperatures: (1) Ni-Al_2O_3-HT at 50 °C; (2) Ni-Al_2O_3-HT at 30 °C; (3) 78 wt% Ni/Al_2O_3-IMP at 30 °C. b) $n(N_2+H_2)/n(N_2H_4)$ versus time for Ni-Al_2O_3-HT at 50 °C: (1) the second time; (2) the fifth time; (3) the tenth time. Inset: magnetic separation of the catalyst after reaction.

After reduction, the major diffraction peak with a 2θ value of 44.5° can be indexed to the (111) plane of fcc Ni (PDF number 01-087-0712). The average particle size of Ni is around 4 nm, based on the Scherrer equation, indicating that the Ni-Al-HT precursor produces a well-dispersed Ni-Al_2O_3-HT catalyst, even with a very high Ni loading of around 78 wt%. Figure 1 b, c show representative HAADF-STEM and HRTEM images of the Ni-Al_2O_3-HT catalyst derived from hydrotalcite. The well-dispersed Ni nanoparticles are surrounded by amorphous alumina (Supporting Information, Figure S1), suggesting they are strongly interacting with the alumina support. This can be further confirmed by the results of H_2-TPR measurement (Supporting Information, Figure S2). The reduction temperature of Ni-Al-HT is notably higher than that of Ni/Al_2O_3-IMP, indicating a much stronger interaction of the Ni component with Al_2O_3 in the former catalyst. The corresponding digital diffraction pattern demonstrates the crystalline nature of these Ni metal nanoparticles. As shown in the size distribution histogram (Figure 1 d), most of the Ni particles are in the range of 3–9 nm, and no particles larger than 10 nm were observed. Among them, 64% of Ni particles are in the range of 3–5 nm. In contrast, the average size of Ni particles of the 78 wt% Ni/Al_2O_3-IMP catalyst is around 38 nm (Supporting Information, Figure S3). The H_2 chemisorption measurement also demonstrates that the Ni-Al_2O_3-HT has a much larger H_2 uptake than the 78 wt% Ni/Al_2O_3-IMP catalyst (702 $\mu mol\,g^{-1}$ vs. 124 $\mu mol\,g^{-1}$), which is in agreement with the conclusions from XRD and HAADF-STEM.

The catalytic performance of the Ni-Al_2O_3-HT catalyst in $N_2H_4{\cdot}H_2O$ decomposition for H_2 generation was examined and compared with the 78 wt% Ni/Al_2O_3-IMP sample. The Ni-Al_2O_3-HT catalyst shows much higher activity and selectivity (Figure 2 a); the reaction was complete within 70 min at 30 °C and the H_2 selectivity was up to 93% (Table 1). In contrast, the 78 wt% Ni/Al_2O_3-IMP catalyst exhibited a much lower activity, with a total reaction time of 440 min. This result is consistent with the poor dispersion of Ni. It should be noted that the H_2 selectivity was only 66%. When the reaction temperature was raised to 50 °C, $N_2H_4{\cdot}H_2O$ was converted completely within 13 min over the Ni-Al_2O_3-HT catalyst and the selectivity still maintained at 93%. Gas chromatographic analysis reveals that the H_2/N_2 molar ratio was 1.95 on the Ni-Al_2O_3-HT and 1.72 on the 78 wt% Ni/Al_2O_3-IMP, respectively, with a corresponding selectivity of 93% and 67% (Supporting Information, Figure S4). This ratio remained constant during the whole reaction process, which is in good agreement with H_2 selectivity obtained from the volumetric observation. On further increasing the reaction temperature from 50 °C to 80 °C, the reaction was complete within 5 min but the selectivity was reduced to 82% (Supporting Information, Table S1), demonstrating that a higher temperature was unfavorable for Reaction (1) but the reaction took place faster than that at lower temperatures. The apparent activation energy for the reaction was about $(49.3 \pm 3.2)\ kJ\,mol^{-1}$ (Supporting Information, Figure S5), which is very similar to the previously reported values for the catalytic decomposition

Table 1: Ni particle size after reduction, catalytic activity and selectivity, and amount of CO_2 desorbed during TPD of the corresponding Ni-Al_2O_3-HT and Ni/Al_2O_3-IMP catalysts.

Catalysts	Reaction temperature [°C]	Average size of Ni [nm]	Reaction time[d] [min]	Selectivity [%]	Total amount of CO_2 desorption [μmol (g Al_2O_3)$^{-1}$]	Strong basic sites [μmol (g Al_2O_3)$^{-1}$]	Weak basic sites [μmol (g Al_2O_3)$^{-1}$]
Ni-Al_2O_3-HT	50	4.0	13	93	414	328	86
Ni-Al_2O_3-HT	30	4.0	70	93	414	328	86
Ni-Al_2O_3-HT (2:1)[a]	30	3.2	64	92	350	259	91
78 wt% Ni/Al_2O_3-IMP	30	38.2	440	66	104	33	71
20 wt% Ni/Al_2O_3-IMP	30	4.0	160	59	166	48	118
K-Ni-Al_2O_3-HT[b]	30	–	86	96	998	845	153
K-20 wt% Ni/Al_2O_3-IMP[c]	30	–	290	76	653	376	277

[a] The molar ratio of Ni/Al was 2:1. [b] The mass percent of K for K-Ni-Al_2O_3-HT was 0.23%. [c] The mass percent of K for K-20 wt% Ni/Al_2O_3-IMP was 2.92%. [d] The time for complete conversion of $N_2H_4{\cdot}H_2O$.

of gaseous N_2H_4.[9] The reaction rate per unit mole of active metal over this Ni-Al_2O_3-HT catalyst was about 2.0 h^{-1}, which is even comparable to the NiPt alloy nanoparticles.[3d] The recyclability of the Ni-Al_2O_3-HT catalyst was also tested. There was no significant decrease in H_2 selectivity from the second to tenth runs (Figure 2b), though the rate of reaction decreased slightly. The slight decrease in reaction rate is due to the formation of small amounts of ammonia rather than the growing crystallite size. Another advantage for potential application is that the catalyst is easily separated from the reaction medium owing to the magnetic property of Ni particles (inset of Figure 2b).

This is the first report that Ni catalyst can catalyze the complete decomposition of $N_2H_4{\cdot}H_2O$ at room temperature. The freshly reduced Ni-Al_2O_3-HT catalyst exhibited desired activity and selectivity for $N_2H_4{\cdot}H_2O$ decomposition, which shows the potential for it to be a candidate to replace noble metals for this reaction. Moreover, the passivated catalyst was totally inactive for this reaction at 30°C. An IR spectrum of adsorbed CO (Supporting Information, Figure S6) shows that for the fresh catalyst, there is a main band appearing at 2059 cm^{-1}, which is typical for CO linear adsorption on metallic Ni; however, there is no CO adsorption observed on the passivated surface, which is probably due to surface oxidation of Ni particles. This result supports the idea that the high catalytic activity of this Ni-Al_2O_3-HT catalyst originates from the metallic Ni.

It should be noted that a much lower H_2 selectivity (only 66%) was observed over the 78 wt% Ni/Al_2O_3-IMP catalyst. We tentatively attribute this to Ni particle size difference (4 nm versus 38 nm), considering that Ni catalysts are structure-sensitive for N–H cleavage in NH_3 decomposition.[10] To confirm this proposition, we prepared a Ni/Al_2O_3-IMP catalyst with a mean particle size of 4 nm by lowering the metal loading to 20 wt%. However, the selectivity to H_2 on the impregnated sample was still very low (around 59%), which is even lower than the 78 wt% Ni/Al_2O_3-IMP catalyst, indicating that the difference in Ni particle size may not be the only reason for the H_2 selectivity. In fact, by varying the molar ratio of Ni/Al and reduction temperature, the particle sizes of Ni-Al_2O_3-HT catalysts can be tuned (Supporting Information, Table S2). Interestingly, there were no significant changes in the selectivity to H_2 when varying the Ni particles size in the range from 3 to 9 nm, while only the reaction rate increased with the reducing of Ni particle size.

A quantitative measure of the number and strength of basic sites was obtained by a CO_2-TPD experiment (Supporting Information, Figure S7 and Table 1). The number of basic sites on Ni-Al_2O_3-HT was clearly larger than that on the impregnated sample. In fact, there are two kinds of basic sites, strong and weak, and the major difference lies in the number of strongly basic sites. By comparing 20 wt% Ni/Al_2O_3-IMP and Ni-Al_2O_3-HT catalysts, which have quite different H_2 selectivity (Supporting Information, Figure S8), we found that the latter catalyst contained many more strong basic sites. Therefore, it is reasonable to speculate that the strong basic sites contribute to the increased H_2 selectivity. To further investigate the influence of the basicity of the catalyst, a small amount of potassium was deliberately introduced to both the Ni-Al_2O_3-HT and Ni/Al_2O_3-IMP catalysts. As expected, the K-promoted catalyst with stronger basicity did exhibit an increase of H_2 selectivity from 93% to 96% for Ni-Al_2O_3-HT and 59% to 76% for Ni/Al_2O_3-IMP. Noticeably, with decreased Ni loading, there was also an increase in the weak basicity of the sample owing to the increased content of Al_2O_3, but this was not accompanied by increase in selectivity.

The decomposition reaction of $N_2H_4{\cdot}H_2O$ consists of several elementary reactions, including the cleavage of N–N and N–H bonds. If the N–N bond firstly breaks to produce $\cdot NH_2$ radical, it is much easier to produce ammonia instead of hydrogen because further N–H bond cleavage needs more energy than the combination of $\cdot NH_2$ and H$\cdot$ to form NH_3.[11] The Ni-Al_2O_3-HT catalyst exhibits much higher selectivity to H_2, which is quite different from other metal catalysts (10% for cobalt, 5% for iridium). This unique selectivity to H_2 can be explained by facilitating the dissociation of N–H bond over Ni-based catalyst.[5b,12] KOH has been reported to be a promoter for selective cracking of the N–H bond in N_2H_4 decomposition.[2e,4] Therefore, the stronger basicity of the Ni-Al_2O_3-HT leads to a highly selective catalyst for production of H_2 from the decomposition of $N_2H_4{\cdot}H_2O$. On the other hand, the selectivity of the Ni-Al_2O_3-HT was significantly higher than that of the K-promoted Ni/Al_2O_3-IMP sample, even though the latter catalyst contained large amounts of strong basic sites. This may be related to the strong metal support interaction (SMSI), as expected from the peculiar textural

property that is typical of hydrotalcite-derived material. Therefore, it is likely that the high H_2 selectivity of Ni-Al_2O_3-HT originates from the cooperative action of the small Ni particle size and strong basic sites located nearby.

In summary, a supported Ni catalyst with a high loading and good dispersion, prepared by using Ni-Al hydrotalcite-like compounds as precursors, exhibits 100% conversion and 93% H_2 selectivity for the decomposition of $N_2H_4{\cdot}H_2O$ at room temperature. This unique catalysis is due to the cooperation of Ni nanoparticles and strong basic sites. This Ni-Al hydrotalcite derived catalyst could be a promising candidate to replace noble metals for the catalytic decomposition of $N_2H_4{\cdot}H_2O$ and for hydrogen generation under ambient conditions.

Received: March 3, 2012
Published online: May 8, 2012

Keywords: basicity · hydrogen storage · hydrazine decomposition · Ni-Al hydrotalcite

[1] a) E. W. Schmidt in *Hydrazine and its Derivatives: Preparation, Properties, Applications*, 2nd ed., Wiley, New York, **2001**; b) H. L. Jiang, S. K. Singh, J. M. Yan, X. B. Zhang, Q. Xu, *ChemSusChem* **2010**, *3*, 541.

[2] a) S. Mary, C. Kappenstein, S. Balcon, S. Rossignol, E. Gengembre, *Appl. Catal. A* **1999**, *182*, 317; b) R. Eloirdi, S. Rossignol, C. Kappenstein, D. Duprez, N. Pillet, *J. Propul. Power* **2003**, *19*, 213; c) X. Chen, T. Zhang, P. Ying, M. Zheng, W. Wu, L. Xia, T. Li, X. Wang, C. Li, *Chem. Commun.* **2002**, 288; d) X. Chen, T. Zhang, M. Zheng, W. Wu, C. Li, *J. Catal.* **2004**, *224*, 473; e) J. Song, R. Ran, Z. Shao, *Int. J. Hydrogen Energy* **2010**, *35*, 7919.

[3] a) S. K. Singh, X.-B. Zhang, Q. Xu, *J. Am. Chem. Soc.* **2009**, *131*, 9894; b) S. K. Singh, Q. Xu, *J. Am. Chem. Soc.* **2009**, *131*, 18032; c) S. K. Singh, Q. Xu, *Chem. Commun.* **2010**, *46*, 6545; d) S. K. Singh, Q. Xu, *Inorg. Chem.* **2010**, *49*, 6148; e) S. K. Singh, Z. H. Lu, Q. Xu, *Eur. J. Inorg. Chem.* **2011**, 2232.

[4] S. K. Singh, A. K. Singh, K. Aranishi, Q. Xu, *J. Am. Chem. Soc.* **2011**, *133*, 19638.

[5] a) W. E. Armstrong, L. B. Ryland, H. H. Voge, US Pat., 4, 124, 538, **1978**; b) M. Zheng, R. Cheng, X. Chen, N. Li, L. Li, X. Wang, T. Zhang, *Int. J. Hydrogen Energy* **2005**, *30*, 1081.

[6] a) L. Wang, J. Liu, Y. Zhou, Y. Song, J. He, D. G. Evans, *Chem. Commun.* **2010**, *46*, 3911; b) M. Zhao, Q. Zhang, W. Zhang, J. Huang, Y. Zhang, D. Su, F. Wei, *J. Am. Chem. Soc.* **2010**, *132*, 14739; c) H. Cheng, Y. Huang, A. Wang, X. Wang, T. Zhang, *Top. Catal.* **2009**, *52*, 1535.

[7] A. Tsyganok, T. Tsunoda, S. Hamakawa, K. Suzuki, K. Takehira, T. Hayakawa, *J. Catal.* **2003**, *213*, 191.

[8] D. G. Tong, X. L. Zeng, W. Chu, D. Wang, P. Wu, *Mater. Res. Bull.* **2010**, *45*, 442.

[9] R. Maurel, J. C. Menezo, J. Barrault, *J. Chim. Phys. Phys.-Chim. Biol.* **1973**, *70*, 1221.

[10] a) J. Zhang, H. Y. Xu, W. Z. Li, *Appl. Catal. A* **2005**, *296*, 257; b) X. Li, W. Ji, J. Zhao, S. Wang, C. Au, *J. Catal.* **2005**, *236*, 181.

[11] a) K. Aika, T. Ohhata, A. Ozaki, *J. Catal.* **1970**, *19*, 140; b) J. L. Gland, G. B. Fisher, G. E. Mitchell, *Chem. Phys. Lett.* **1985**, *119*, 89; c) P. Zhang, Y. Wang, Y. Huang, T. Zhang, G. Wu, J. Li, *Catal. Today* **2011**, *165*, 80.

[12] a) Y. K. Al-Haydari, J. M. Saleh, M. H. Matloob, *J. Phys. Chem.* **1985**, *89*, 3286; b) D. J. Alberas, J. Kiss, Z. M. Liu, J. M. White, *Surf. Sci.* **1992**, *278*, 51.

